Antitumor Efficacy of the Novel RAF Inhibitor GDC-0879 Is Predicted by BRAF^{V600E} Mutational Status and Sustained Extracellular Signal-Regulated Kinase/Mitogen-Activated Protein Kinase Pathway Suppression

Klaus P. Hoeflich,[1] Sylvia Herter,[1] Janet Tien,[1] Leo Wong,[1] Leanne Berry,[1] Jocelyn Chan,[1] Carol O'Brien,[2] Zora Modrusan,[3] Somasekar Seshagiri,[3] Mark Lackner,[2] Howard Stern,[4] Edna Choo,[5] Lesley Murray,[1,5] Lori S. Friedman,[1] and Marcia Belvin[1]

Departments of [1]Cancer Signaling and Translational Oncology, [2]Molecular Diagnostics, [3]Molecular Biology, [4]Pathology, and [5]Drug Metabolism and Pharmacokinetics, Genentech, Inc., South San Francisco, California

Abstract

Oncogenic activation of the BRAF serine/threonine kinase has been associated with initiation and maintenance of melanoma tumors. As such, development of pharmacologic agents to target RAF proteins or their effector kinases is an area of intense investigation. Here we report the biological properties of GDC-0879, a highly selective, potent, and orally bioavailable RAF small-molecule inhibitor. We used extracellular signal-regulated kinase (ERK)-1/2 and mitogen-activated protein kinase/ERK kinase (MEK)-1/2 phosphorylation as biomarkers to explore the relationship between tumor outcome and pharmacodynamic inhibition of the RAF-MEK-ERK pathway. In GDC-0879–treated mice, both cell line– and patient-derived BRAF^{V600E} tumors exhibited stronger and more sustained pharmacodynamic inhibition (>90% for 8 hours) and improved survival compared with mutant KRAS–expressing tumors. Despite the involvement of activated RAF signaling in RAS-induced tumorigenesis, decreased time to progression was observed for some KRAS-mutant tumors following GDC-0879 administration. Moreover, striking differences were noted for RAF and MEK inhibition across a panel of 130 tumor cell lines. Whereas GDC-0879–mediated efficacy was associated strictly with BRAF^{V600E} status, MEK inhibition also attenuated proliferation and tumor growth of cell lines expressing wild-type BRAF (81% KRAS mutant, 38% KRAS wild type). The responsiveness of BRAF^{V600E} melanoma cells to GDC-0879 could be dramatically altered by pharmacologic and genetic modulation of phosphatidylinositol 3-kinase pathway activity. These data suggest that GDC-0879–induced signaling changes are dependent on the point of oncogenic activation within the RAS network. Taken together, these studies increase our understanding of the molecular determinants for antitumor efficacy resulting from RAF pathway inhibition and have implications for therapeutic intervention in the clinic. [Cancer Res 2009;69(7):3042–51]

Introduction

RAF protein kinases have been implicated in cellular responses relevant to tumorigenesis, including cell proliferation, invasion, survival, and angiogenesis (1, 2). The RAF family is composed of three members, ARAF, BRAF, and RAF1, which play a pivotal role in transducing signals from RAS to downstream kinases, mitogen-activated protein kinase (MAPK)/extracellular signal-regulated kinase (ERK) kinase (MEK)-1/2 and ERK-1/2. Activating somatic mutations in BRAF are frequently observed in several tumor types, including malignant melanoma (3) and colorectal carcinoma (4). Almost 90% of these BRAF mutations are a T1799A transversion in exon 15 that results in a Val^{600}Glu (V600E) amino acid substitution in the activation segment of the kinase. This mutation obviates the requirement for the Thr599 and Ser602 phosphorylation that occurs during normal BRAF activation and leads to constitutive kinase activity that is 500-fold greater than that of wild-type protein (5, 6). In melanoma, BRAF mutation has been reported in premalignant atypical or dysplastic nevi and may thereby implicate BRAF activation as an initiating event in tumorigenesis (7). Tumor maintenance of melanoma cell lines *in vivo* is also highly dependent on BRAF^{V600E} (8, 9). Experiments with BRAF-specific inducible short hairpin RNA (shRNA) show that BRAF^{V600E} silencing in an established tumor inhibits further tumor progression, and in some tumor xenograft models the loss of BRAF^{V600E} resulted in complete tumor regression (9). This effect was caused by loss of proliferation, increased apoptosis, and macrophage infiltration. Taken together, BRAF represents an excellent target for anticancer therapy based on epidemiology, preclinical target validation, and drugability of protein kinases.

There are currently numerous efforts to develop therapeutic agents to target BRAF or its downstream kinases (10). The first RAF inhibitor to enter clinical development was the multikinase inhibitor Nexavar (sorafenib tosylate), which is now approved for the treatment of patients with advanced renal cell carcinoma and unresectable hepatocellular carcinoma. However, the broad selectivity profile of this inhibitor makes it unsuitable for proof-of-concept evaluation of RAF kinase inhibition in tumors (11). Recently, more selective RAF inhibitors have been disclosed, and chemical inhibition of BRAF enzymatic activity using these compounds can result in diminished proliferation and survival of tumor cells *in vitro* (12, 13). However, only very limited *in vivo* data have been published for these inhibitors. For instance, daily administration of SB-590885 resulted in a slight delay of tumor growth for one BRAF-mutant melanoma xenograft model (12). This effect was consistent with the modest reduction (50–80%) in

Note: Supplementary data for this article are available at Cancer Research Online (http://cancerres.aacrjournals.org/).

Requests for reprints: Marcia Belvin, Genentech, Inc., 1 DNA Way, South San Francisco, CA 94080. Phone: 650-467-7346; Fax: 650-225-1411; E-mail: mbelvin@gene.com or Lori Friedman, Phone: 650-467-1926; E-mail: lorif@gene.com.

doi:10.1158/0008-5472.CAN-08-3563

phospho-ERK levels observed in tumors for this compound. P.o. administration of another compound, PLX4720, was shown to be very efficacious in two $BRAF^{V600E}$ tumor models; however, there was no suggestion of the kinetics or magnitude of downstream pathway modulation that was required for antitumor efficacy (13).

Clearly, a more extensive preclinical validation of RAF inhibitors in tumors of varying genotypes and a thorough pharmacodynamic characterization of pathway inhibition are essential to achieving the important goal of targeting RAF signaling for clinical benefit while maintaining a significant therapeutic window. As such, novel small-molecule antagonists to inhibit RAF enzymatic activity were synthesized (14), and here we describe the biological effects of two highly selective molecules with excellent potency and oral bioavailability, GDC-0879 and compound 2a. GDC-0879 was used to explore the dependency of cell lines and tumors with BRAF or KRAS mutant genotypes on phospho-ERK signaling to maintain cellular proliferation and tumor growth. GDC-0879 and compound 2a were also tested for antitumor efficacy in a large panel of xenograft models derived from either cell lines or primary human tumors and their efficacy correlated with pharmacodynamic end points *in vivo*.

Materials and Methods

Reagents. All cell lines were acquired from American Type Culture Collection and maintained at 37°C and 5% CO_2 in DMEM or RPMI 1640 with 10% fetal bovine serum, 4 mmol/L L-glutamine, and penicillin-streptomycin. Nontargeting and phosphatase and tensin homologue (PTEN)–specific small interfering RNAs (siRNA) were obtained from Dharmacon. Antibodies used for immunoblotting were as follows: anti–phospho-ERK1/2 (Thr202/Tyr204), anti-ERK1/2, anti–phospho-MEK1/2 (Ser217/221), anti-MEK1, and anti–β-actin (Cell Signaling Technology) and horseradish peroxidase (HRP)–conjugated secondary antibodies (Pierce Biotechnology). Doxycyline-HCl was purchased from BD Biosciences. Compound 2a, GDC-0879, and sorafenib were administered as a suspension in 0.5% methylcellulose 0.2% Tween 80 (MCT) at a concentration of 10 mg/mL. Dosing solutions were prepared once per week and stored at 4°C.

Cell viability assays. Cells were seeded at 2,000 per well in 384-well plates overnight. On day 2, nine serial 1:2 compound dilutions were made in DMSO in a 96-well plate. The compounds were further diluted into growth media using a Rapidplate robot (Zymark Corp.). The diluted compounds were then added to quadruplicate wells in 384-well cell plates and incubated at 37°C and 5% CO_2. After 4 d, the relative numbers of viable cells were measured by luminescence using CellTiter-Glo (Promega) according to the manufacturer's instructions and read on a Wallac Multilabel Reader (Perkin-Elmer). EC_{50} values were calculated using Prism 4.0 software (GraphPad). Combination assays were dosed starting at $4\times$ EC_{50} drug concentrations. GDC-0879 and GDC-0941 were added simultaneously. For synergy calculations, the combination index between GDC-0879 and GDC-0941 was assessed by the method of Chou and Talalay using Calcusyn software (Biosoft). Combination index values <0.4 indicate a synergistic inhibition of cell viability.

Immunoblotting and ELISA. Frozen tumors were pulverized on dry ice using a small Bessman tissue pulverizer (Spectrum Laboratories, Inc.) and protein extracts were prepared at 4°C with Cell Lysis Buffer (Cell Signaling Technology), 1 mmol/L phenylmethylsulfonyl fluoride (Sigma-Aldrich), and one tablet of Complete Mini protease inhibitor cocktail (Roche Diagnostics). Tissue lysates were subjected to centrifugation at 16,100 × *g* for 30 min and protein concentration was determined using the Bradford method (Bradford 1976). ELISA kits were used to determine levels of phosphorylated and total MEK1 in 96-well format (Biosource International) and samples were analyzed in duplicate at 75 mg protein/well according to the manufacturer's protocol. The absorbances obtained at 450 nm were converted to units per milliliter (phospho-MEK1) or nanograms per milliliter (total MEK1) using a standard curve determined with recombinant proteins. The phospho-MEK1/total MEK1 ratios were then calculated as units per nanogram.

For Western blot analysis, tumor protein extracts were prepared from frozen tumors as described above. Proteins were resolved by 10% SDS-PAGE and transferred onto polyvinylidene difluoride membranes (Millipore Corp.). Total and phosphorylated ERK1/2 (Thr202/Tyr204) and β-actin were detected with rabbit polyclonal antibodies (Cell Signaling Technology).

Microarray analysis and statistical methods. A375 cells were treated with 10 μmol/L of compound 2a, GDC-0879, or sorafenib for 24 h. Cells cultured in regular medium were used as a control. Inducible shRNA A375 cell clones have been described previously (9) and were treated with 1 mg/mL doxycycline for 3 d. Total RNA was isolated using the RNeasy RNA isolation kit (Qiagen) from at least two independent cell cultures. Complementary RNA was synthesized and hybridized to Affymetrix human genome 133 Plus 2.0 arrays (HGU133P). For all probe sets, an ANOVA was applied to estimate the expression and accompanying variability for each of the treatment groups. Additionally, fold change estimates for treated versus untreated cultures were computed. The Benjamini and Hochberg false discovery rate was applied as a multiple test correction. Gene ontologies were assigned using the information provided by the Gene Ontology Consortium.[6]

Tumor xenograft models. Cultured cells were resuspended in PBS, mixed 1:1 with Matrigel (BD Biosciences), and were implanted s.c. into the right flank of naïve female *nu/nu* mice. Mice with tumors of a mean volume of 200 to 250 mm^3 were grouped into treatment cohorts. For *in vivo* studies done at Oncotest GmbH, tumor fragments obtained from MEXF 274, MEXF 535, MEXF 1341, MEXF 989, MEXF 276, MEXF 514, LXFA 629, LXFA 983, and LXFA 1041 xenografts in serial passage were cut into 1- to 2-mm pieces and placed in RPMI 1640 until bilateral, s.c. implantation into NMRI *nu/nu* mice (Taconic). When tumors reached an average of 100 mm^3, animals were stratified into two equivalent groups of 10 tumor-bearing mice.

RAF inhibitors were formulated in 0.5% methylcellulose/0.2% Tween 80 and administered daily by oral gavage. Body weights and caliper measurements were taken twice per week during the study. Tumor volumes were calculated by the following formula: Tumor Volume = $0.5 \times (a \times b^2)$, where a is the largest tumor diameter and b is the perpendicular tumor diameter. Tumor volume results are presented as mean tumor volume ± SE. Percent growth inhibition at the end of study (EOS) was calculated as %INH = 100 × [(EOS Vehicle − EOS Treatment) / (EOS Vehicle)]. Data analysis and generation of P values using the Dunnett t test (15) was done using JMP software.

Immunohistochemistry. Xenograft tissues were fixed for 24 h in 10% neutral buffered formalin and were then processed and paraffin embedded. Sections were cut at a thickness of 3 μm, and specimens with sufficient viable tumor (assessed on H&E-stained slides) were further evaluated by immunohistochemistry. Anti–Ki-67 (clone MIB-1, mouse anti-human) was used with the DAKO ARK Kit for detection. Anti–panendothelial cell marker (clone MECA-32, monoclonal rat anti-mouse) and anti–phospho-MAPK Thr202/Tyr204 (clone 20G11, monoclonal rabbit anti-human) were both used with a standard avidin-biotin HRP detection system. Tissues were counterstained with hematoxylin, dehydrated, and mounted. In all cases, antigen retrieval was done with the DAKO Target Retrieval Kit as per manufacturer's instructions.

For quantification of immunohistochemically Ki-67–positive cells, images were acquired by the Ariol SL-50 automated slide-scanning platform (Genetix Ltd.) at ×100 final magnification, and tumor-specific areas were identified manually for analysis in the Ariol software. A 3,3′-diaminobenzidine–specific color range was specified using the hue, saturation, and intensity color space to quantify the area of staining and the output was total Ki-67–positive cells in relation to total cell count. To analyze Ariol scanned images of MECA-32, tumor-specific areas were exported for analysis in the Metamorph software package (MDS Analytical Technologies) as individual 8-bit images. A segmentation algorithm identified vessels and

[6] http://www.geneontology.org

removed noise based on size and shape. Cells were identified as either tumor or nontumor based on size, shape, and density of hematoxylin staining. Area measurements are logged for individual vessels, as well as the tumor and nontumor areas in each image.

Results

GDC-0879 is a potent and selective RAF kinase inhibitor. Medicinal chemistry efforts generated a series of compounds based on a substituted pyrazole core to produce ATP-competitive RAF kinase inhibitors with excellent potency and physiochemical properties (14). In particular, GDC-0879 and compound 2a (Fig. 1*A*) show significant, equipotent inhibition of wild-type BRAF, $BRAF^{V600E}$, and CRAF as determined by *in vitro* inhibition of purified enzymes (14). For both compounds, subnanomolar enzyme potency translated into very effective reduction of phospho-ERK levels (compound 2a and GDC-0879 IC_{50} values were 33 and 63 nmol/L, respectively) and cellular viability of BRAF-mutant Malme3M cells (EC_{50} values were 0.46 and 0.75 μmol/L for compound 2a and GDC-0879, respectively).

To determine the selectivity profile of these RAF inhibitors across a larger fraction of the kinome, GDC-0879 was screened against a panel of 140 full-length protein kinases at a final concentration of 1 μmol/L. In these assays, RAF kinases were inhibited by >90% and only one additional kinase, casein kinase-1δ, showed >50% inhibition *in vitro* (Supplementary Table S1). Moreover, we assessed changes in global gene expression of $BRAF^{V600E}$ A375 melanoma cells in response to treatment with 10 μmol/L of GDC-0879, compound 2a, or sorafenib for 24 hours. As a comparator, we used the previously described tetracycline-inducible shRNA expression system to achieve conditional and selective genetic knockdown of BRAF in A375 cells (9). Encouragingly, unsupervised hierarchical clustering revealed a strong similarity in gene modulation resulting from either treatment with compound 2a or GDC-0879 or genetic ablation of BRAF mediated by RNA interference relative to DMSO-treated control samples (Fig. 1*B*). We further analyzed these changes by testing their association with the biological processes arrayed in the Gene Ontology database. Genes most significantly down-regulated by selective RAF inhibition were strongly associated with cell proliferation (Supplementary Table S2). Given the numerous kinases that are inhibited by sorafenib, it was not unexpected that gene expression induced by this compound differed considerably from that of the RAF-specific reagents. Taken together, these data show the remarkable kinase specificity of GDC-0879 and compound 2a and support the use of these inhibitors in further investigations of RAF signaling and biology.

The inhibition of MEK1/2 phosphorylation on the key activation segment residues S217/221 was also determined for this chemical series using a small panel of tumor cell lines. Representative GDC-0879 dose-response curves for phospho-MEK are shown for A375 ($BRAF^{V600E}$ melanoma), A2058 ($BRAF^{V600E}$ melanoma), and HCT116 ($KRAS^{G13D}$ colon cancer) cells in culture (Fig. 1*C*). It was noted that inhibition of MEK-ERK signaling was attenuated in the KRAS-mutant cell line relative to tumor cells in which pathway activation was induced directly by oncogenic BRAF. This observation led us to investigate the GDC-0879 responsiveness of a larger panel of BRAF-, KRAS-, and NRAS-mutant tumor cell lines.

Cellular activity of GDC-0879 on tumor cell lines expressing oncogenic BRAF or RAS. The potency of GDC-0879 for a panel of melanoma, colorectal, and non–small-cell lung cancer cell lines is shown in Fig. 2. The cell lines were further classified according to their *BRAF, KRAS*, and *NRAS* genotypes. Tumor cells with oncogenic mutations in either KRAS or NRAS showed limited dependence on BRAF activity and were frequently resistant to GDC-0879 treatment *in vitro* (EC_{50} > 7.5 μmol/L for 28 of 32 cell lines). However, there was a good correlation between GDC-0879 sensitivity and activating mutations in the *BRAF* oncogene. Cells with GDC-0879 EC_{50} values <0.5 μmol/L all express V600E oncogenic alleles for *BRAF* (A375, 624, SK-MEL-28, Malme3M, C32, 928, 888, G-361, Colo205, Colo206, SW1417, CL34, and Colo201). Moreover, few BRAF-mutant cell lines were highly resistant to RAF inhibition. Of these resistant cell lines, HT-55 and H2405 carry atypical, and as yet uncharacterized, genetic aberrations within the BRAF gene (N581Y and L485Y, respectively). $BRAF^{V600E}$ mutant HT29 cells were unexpectedly insensitive to GDC-0879 (Fig. 2). However, HT29 cells have been shown to exhibit high UDP-glucuronosyltransferase activity (16), and drug conjugation catalyzed by UDP-glucuronosyltransferases might function as an intrinsic mechanism of resistance to GDC-0879 in some cell lines. Lastly, although relatively weak *in vitro* activity was observed for $BRAF^{V600E}$ LOX-IMVI melanoma cells in culture (10 μmol/L), dramatic *in vivo* efficacy was observed using tumor xenografts derived from this cell line (Supplementary Table S3).

Although little is known about resistance mechanisms for RAF inhibitors, compensatory signaling through the phosphatidylinositol 3-kinase (PI3K)-AKT pathway has recently been suggested to underlie genetic resistance to BRAF-MEK inhibitors in some cases (17). Because AKT activation can occur as a result of activating mutations in PIK3CA or loss of the PTEN tumor suppressor, we carefully examined the mutational status of these genes in our collection of BRAF-mutant cell lines. In no instances did $BRAF^{V600E}$ cell lines that were highly sensitive to GDC-0879 have either established hotspot mutations of PIK3CA (E545K, H1047R) or loss of PTEN protein as determined by immunoblotting with a PTEN-specific antibody (data not shown). In contrast, some cell lines with considerably less dependence on BRAF activity for proliferation (A2058, RPMI-7951, RKO-AS45-1, and RKO) carried mutations predicted to deregulate PI3K signaling (data not shown). DNA sequencing of RKO-AS45-1 and RKO cells (EC_{50} values of 1.16 and 9.16 μmol/L, respectively) revealed $PIK3CA^{H1047R}$ driver mutations. Furthermore, A2058 and RPMI-7951 melanoma cells (EC_{50} values of 7 and 20 μmol/L, respectively) were confirmed to contain large deletions within the *PTEN* gene. Consistent with this hypothesis, combined treatment of A2058 ($BRAF^{V600E}$, $PTEN^{-/-}$) cells with GDC-0879 and GDC-0941, a highly selective and potent inhibitor of class I PI3Ks that is currently in phase I clinical testing (18), resulted in synergistic inhibition of cell proliferation over a broad range of drug concentrations as determined by the Chou and Talalay method of combination index (combination index = 0.23, $P < 0.0001$; Fig. 2*B*). PI3K signaling was also induced via genetic ablation of PTEN in a GDC-0879–sensitive cell line, MDA-MB-435S ($BRAF^{V600E}$) melanoma cells (19). Elevated PI3K signaling resulted in significant resistance to GDC-0879–mediated inhibition of cell proliferation ($P < 0.0001$; Fig. 2*C*). Comparable PTEN knockdown results were observed for distinct siRNA duplexes, and GDC-0879 resistance was evident over a wide range of GDC-0879 concentrations. Moreover, inhibition of basal PI3K signaling via dual knockdown of PIK3CA and PIK3CB sensitized cells to GDC-0879 ($P < 0.0001$). Taken together, our cellular data suggest that positive (BRAF mutation) and potential negative (PIK3CA and PTEN mutation) predictors of response to the RAF inhibitors can be identified.

GDC-0879 and compound 2a are highly efficacious in $BRAF^{V600E}$ tumor xenograft models. The key physical properties of GDC-0879 and compound 2a, such as hydrophilicity and solubility at neutral pH, result in good pharmacokinetic profiles and high exposure of these compounds in several preclinical species (data not shown). For instance, following p.o. administration of 25 mg/kg GDC-0879 to CD-1 mice, the maximum plasma concentration reached 5.5 μg/mL and the drug half-life in plasma was 3.8 hours. Area under the plasma concentration time curve increased linearly with dose, and bioavailability was estimated to range between 49% and 65%. From these data, it is predicted that efficacious exposure levels of GDC-0879 and compound 2a are attainable and that these compounds can be used for validation of RAF catalytic activity for the maintenance of tumors *in vivo*.

To extend our *in vitro* observations, the breadth of GDC-0879 and compound 2a antitumor activity was evaluated using flank xenograft models established from human tumor cell lines of known BRAF and KRAS mutation status. We implanted a panel of melanoma, colon, lung, and pancreatic cancer cell lines (n = 9) in nude mice. Following tumor establishment (200–250 mm^3), animals were dosed once daily with 100 mg/kg GDC-0879 by oral gavage and tumor growth was monitored by caliper measurement. As shown in Supplementary Table S3, administration of a selective RAF inhibitor prevented tumor growth exclusively in cell line–derived tumor xenografts that were $BRAF^{V600E}$ mutant. Daily treatment for 21 consecutive days induced significant tumor responses in LOX-IMVI, A375, and Colo205 xenografts (93%, 85%, and 53% tumor inhibition, respectively). Rapid tumor regression was observed for the majority of LOX-IMVI tumor–bearing mice and complete responses (regression of the established tumor beyond the level of detection by palpation) or partial responses (shrinkage of at least 50% relative to starting tumor volume) were observed in 10% and 70% of the animals, respectively. Chronic GDC-0879 treatment was well tolerated with minimal body weight loss at this dose, and only mild skin acanthosis and hyperkeratosis were noted on histologic examination. None of the examined xenograft models that were wild-type for BRAF showed tumor inhibition exceeding ~10%, further supporting that *in vivo* efficacy of GDC-0879 correlates well with cellular activity.

To more closely investigate the activity and cellular mechanism of action within sensitive tumor types, compound 2a was benchmarked against sorafenib using $BRAF^{V600E}$ LOX-IMVI tumor

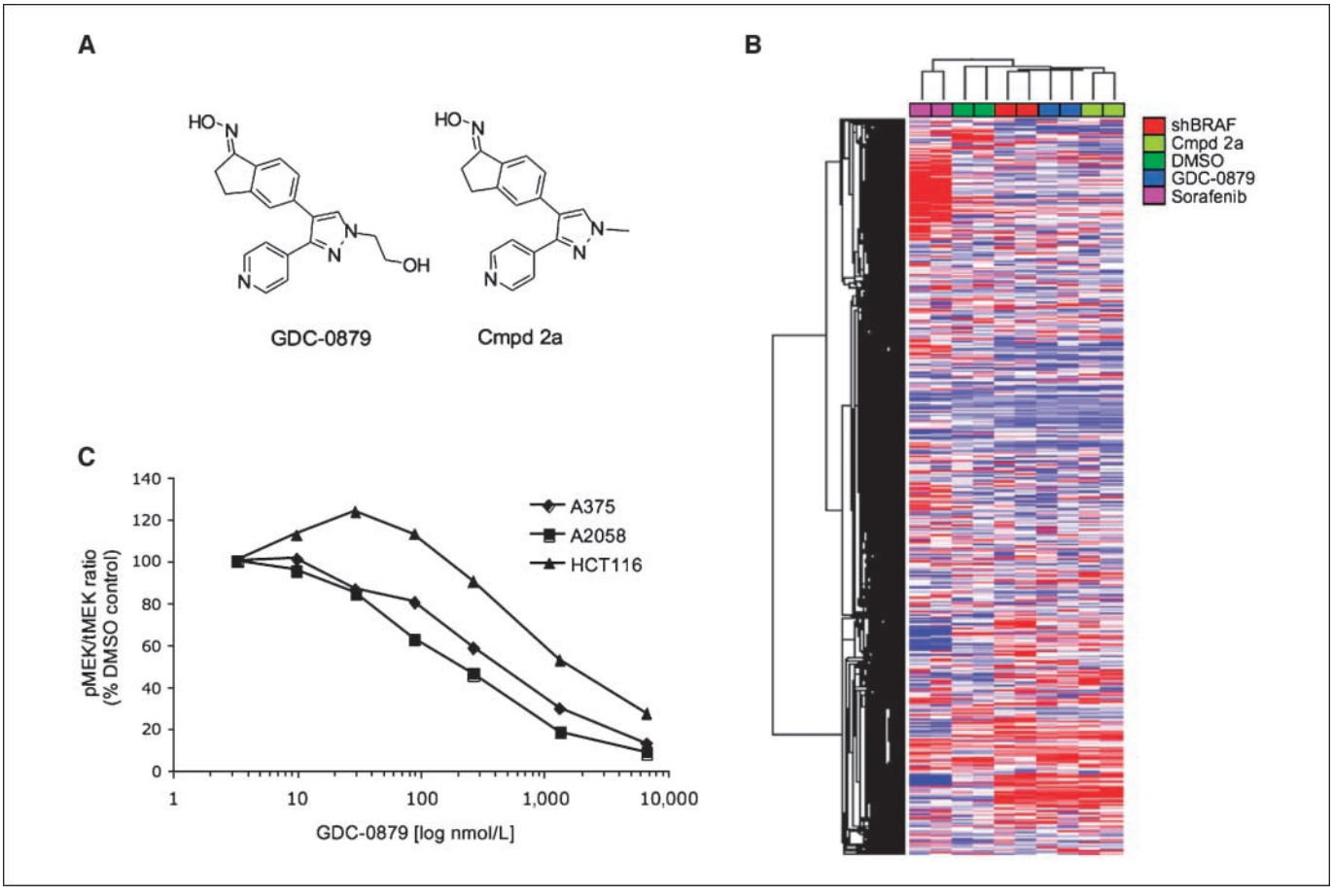

Figure 1. GDC-0879 is a potent and selective RAF kinase inhibitor. *A,* chemical structures of GDC-0879 and compound 2a (*Cmpd 2a*). Both compounds potently inhibit $BRAF^{V600E}$ enzymatic activity and phosphorylated ERK1/2 levels in Malme3M cells. *B,* dendrogram and clustered heat map depicting relatedness of global gene expression profiles resulting from BRAF inhibition via either small-molecule treatment (GDC-0879, compound 2a, or sorafenib) or shRNA-mediated knockdown. Each column represents an independent RNA sample. *Red* and *blue,* high and low expression levels, respectively. The expression profiles of compound 2a and GDC-0879 are similar to the signature obtained by genetic ablation of BRAF. *C,* dose-dependent decrease of RAF effector signaling induced by GDC-0879 was quantified by phosphorylated MEK1 (*pMEK*) normalized to total MEK1 (*tMEK*) in A375 (*diamond*), A2058 (*square*), and HCT116 (*triangle*) cells. Representative of three replicate experiments.

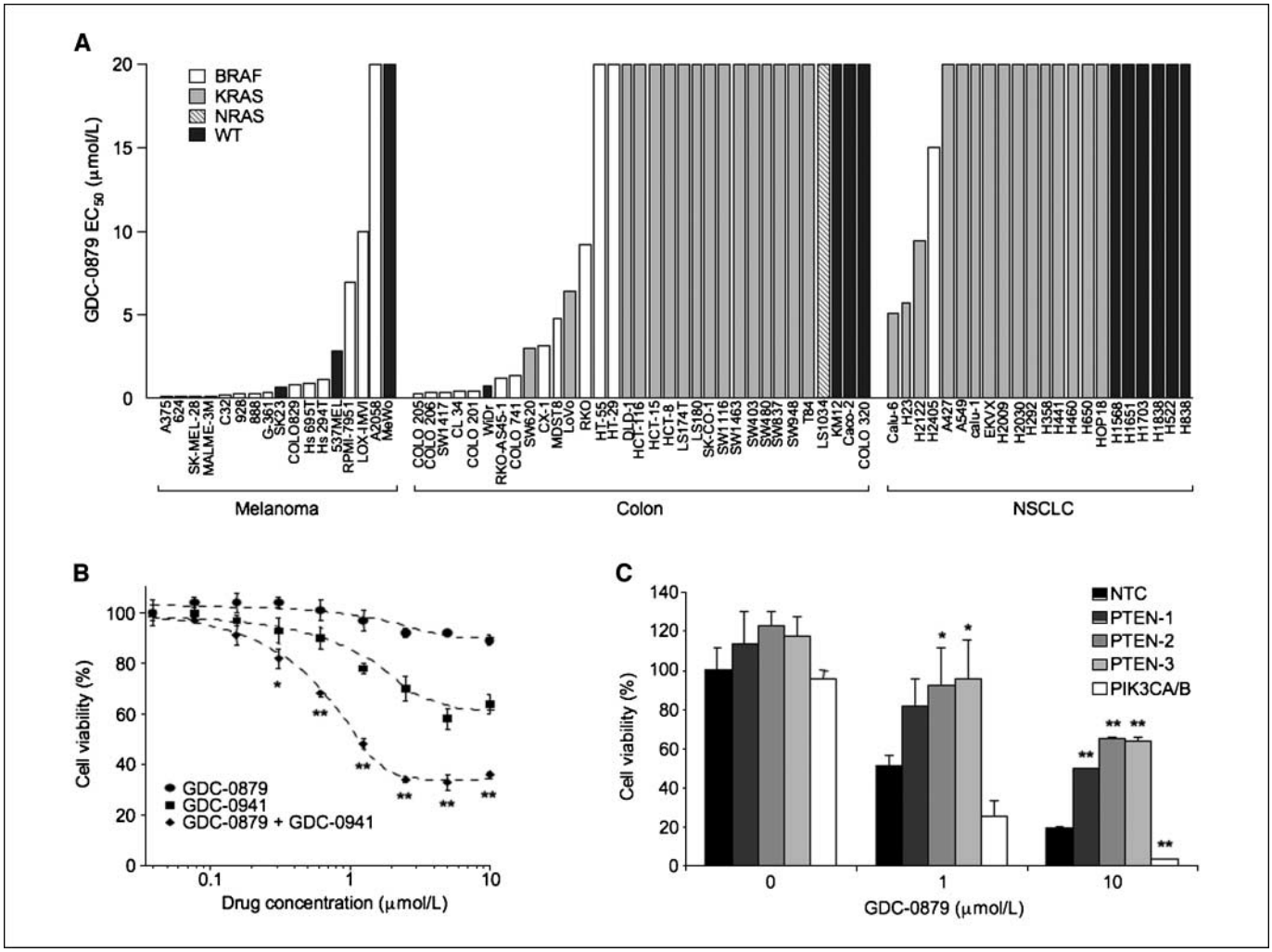

Figure 2. $BRAF^{V600E}$ mutation predicts for enhanced sensitivity of melanoma, colon, and lung cancer cell lines to RAF inhibitors *in vitro. A,* GDC-0879 EC_{50} values were determined for a panel of human tumor cell lines. Cell lines were also assessed for RAS-RAF genotype: BRAF mutation (*white*), KRAS mutation (*light gray*), NRAS mutation (*hatched*), and wild-type (*WT*; *dark gray*). *B,* inhibition of PI3K sensitizes GDC-0879–resistant melanoma cells to RAF inhibition. A2058 ($BRAF^{V600E}$, $PTEN^{-/-}$) melanoma cells were treated with RAF inhibitor (GDC-0879), PI3K inhibitor (GDC-0941), or the combination of the two compounds. The highest concentration of each drug was 4× EC_{50} of each compound, and 2-fold serial dilutions were assessed in an eight-point dilution curve. Cells were incubated in the presence of compounds for 4 d and analyzed by a CellTiter-Glo viability assay. All treatments were done in quadruplicate. A significant combinatorial activity was observed (*, $P < 0.01$; **, $P < 0.0001$, Student's *t* test). *C,* PTEN knockdown induces GDC-0879 resistance in mutant BRAF–expressing cells. MDA-MB-435S ($BRAF^{V600E}$) melanoma cells were transfected with 100 nmol/L siRNA for 72 h before treatment with 0, 1, or 10 μmol/L of GDC-0879 for an additional 72 h. Nontarget control (*NTC*), PTEN, and PIK3CA/PIK3CB siRNA duplexes (*PIK3CA/B*) were used as indicated. Cellular viability was determined by CellTiter-Glo assay and normalized to untreated, NTC-transfected cells. PTEN knockdown using distinct siRNA duplexes resulted in significant resistance to GDC-0879 compared with NTC-transfected cells treated with either 1 or 10 μmol/L GDC-0879 (*, $P < 0.05$; **, $P < 0.0001$, Student's *t* test). In contrast, combined knockdown of PIK3CA and PIK3CB sensitized cells to GDC-0879. All treatments were done in duplicate. *Columns,* mean; *bars,* SE.

xenografts (Fig. 3*A*). Both compounds were administered p.o. at equivalent doses (50 mg/kg daily) and suitable plasma exposure was achieved (4.2 ± 0.6 and 23 ± 12.8 μmol/L at 1 hour after last dose for compound 2a and sorafenib, respectively). Antitumor efficacy was durable throughout the dosing period and the observed tumor inhibition was significantly greater for compound 2a (66.5%, $P = 0.0011$) than for sorafenib (38.7%, $P = 0.0438$) relative to vehicle-treated cohorts. Moreover, tumors that were collected from mice dosed for 4 days revealed that only compound 2a treatment was accompanied by a robust decrease in proliferating cells as determined by Ki-67 immunoreactivity in tumors (Fig. 3*B* and *C*). Compound 2a treatment did not play a pivotal role in regulating vascularization of $BRAF^{V600E}$ tumors as determined by staining with the panendothelial cell marker, MECA-32 (Fig. 3*B* and *D*). In comparison, sorafenib treatment did not affect the proliferative index of the tumor but rather led to a reduction of tumor vascular density (possibly via inhibition of receptor tyrosine kinase signaling; ref. 11). No differences for tumor cell apoptosis were noted at day 4 for either inhibitor as determined by cleaved caspase-3 staining (data not shown). Taken together, these results provide substantial *in vivo* support of the current view that RAF family signaling and catalytic activity are important for driving tumor cell proliferation and suggest a unique mechanism of action compared with some published inhibitors, such as sorafenib.

Pharmacodynamic analysis of GDC-0879 in tumors. Given that the tumor response exhibited by GDC-0879 treatment correlated with the BRAF genotype of the xenograft model

(Supplementary Table S3), A375 ($BRAF^{V600E}$) and SK23 (BRAF wild-type) melanoma xenograft models were used as comparators to evaluate the relationship between *in vivo* efficacy and pharmacodynamic modulation of RAF effector signaling. Daily p.o. administration of 50 or 100 mg/kg GDC-0879 yielded 65% and 85% inhibition of tumor volumes relative to vehicle-treated A375 tumors (Fig. 4*A*). The observed efficacy was significantly less for SK23 tumors, although the pharmacokinetic profile of plasma drug concentration was comparable between xenograft models (Fig. 4*B*; data not shown). In parallel to these efficacy experiments, additional cohorts of A375 and SK23 tumor-bearing mice were treated with a single dose of vehicle or 100 mg/kg GDC-0879. Tumor tissue was subsequently harvested at 1, 4, 8, 12, or 24 hours as indicated (Fig. 4*C* and *D*). Administration of GDC-0879 resulted in profound pathway modulation in A375 tumors collected at early time points (13 $\pm$ 4% and 28 $\pm$ 17% activity remaining at 1 and 4 hours post-dose, respectively) as determined by measurement of MEK1 phosphorylation of Ser217/221 (Fig. 4*C*). Reduced levels of phospho-MEK1 were still evident 8 hours post-dose (59 $\pm$ 21%) but returned to baseline after 12 hours. In comparison, pharmacodynamic analysis of SK23 tumors revealed only modest, variable inhibition of phospho-MEK1 levels at 1, 4, and 8 hours, although baseline MEK1 phosphorylation was equivalent to that of A375 tumors (Fig. 4*D*). Western blot analysis of ERK1/2 phosphorylation (Thr202/Tyr204) further confirmed that significant, sustained pharmacodynamic modulation occurred in A375, but not SK23, tumors (Fig. 4*C* and *D*). As a control, no differences were noted for total ERK1/2 or actin protein levels in this experiment. Moreover, the kinetics of phospho-ERK inhibition determined by immunohistochemical analysis of A375 tumors were also in agreement with results obtained from whole tumor lysates (Supplementary Fig. S1*A*). Despite the transient pharmacodynamic modulation observed for daily dosing, GDC-0879 administration over consecutive days resulted in sustained inhibition of A375 tumor cell proliferation as determined by Ki-67 immunohistochemistry at 4 and 24 hours post-dose (Supplementary Fig. S1*B*). Taken together, the magnitude and duration of phospho-MEK and phospho-ERK reduction correlated well with antitumor efficacy resulting from inhibition of RAF catalytic activity in cell line–derived melanoma xenograft models.

The pharmacodynamics-efficacy relationship for RAF inhibition was further evaluated using human tumors that have been transplanted and passaged directly in athymic mice. In contrast to cell line–derived tumors, these primary tumor xenografts maintain their original tumor histology and are considered to have molecular characteristics and drug sensitivities that better mirror the original patient tumor (20). For our experiments, six patient-derived melanomas and three patient-derived non–small-cell lung adenocarcinomas were genotyped for RAS/BRAF activating mutations and used for GDC-0879 *in vivo* studies. As would be predicted from our previous experiments, tumors with wild-type alleles of BRAF were resistant to GDC-0879 (Supplementary Table S4). However, patient-derived $BRAF^{V600E}$ melanomas were highly sensitive to RAF inhibition and either tumor stasis (MEXF 514) or partial regression (MEXF 989, MEXF 276) was observed. GDC-0879 efficacy for $BRAF^{V600E}$ tumors was significant ($P < 0.0001$) when analyzed as time to tumor progression from Kaplan-Meier curves (Fig. 5*A*). Although NRAS has also been suggested to be an initiating event in melanoma tumor formation and is known to signal strongly through RAF kinases, only a slight delay ($P = 0.01$) in tumor growth was noted for one $NRAS^{Q61K}$ model (MEXF 535) treated with GDC-0879. This suggests that RAF inhibition may not

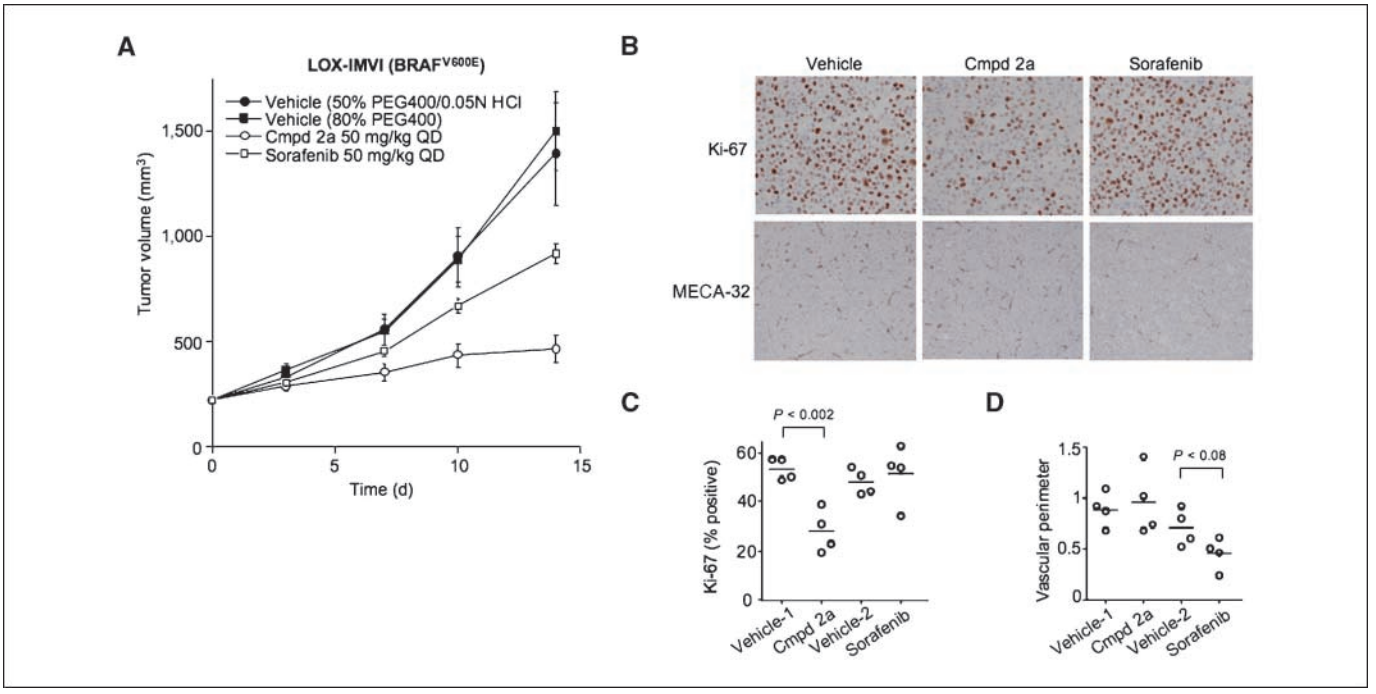

Figure 3. The compound 2a *in vivo* mechanism of action differs from that of sorafenib in $BRAF^{V600E}$ melanoma tumor xenografts. *A, in vivo* activity of compound 2a (*open circle*) and sorafenib (*open square*). Significant inhibition of LOX-IMVI tumor growth was observed for compound 2a relative to vehicle control (*black circle*). *Points,* mean for at least 10 animals; *bars,* SE. *B,* histologic analysis of LOX-IMVI tumors treated with compound 2a or sorafenib. LOX-IMVI tumor–bearing mice were dosed daily with 50 mg/kg of either compound and sacrificed on day 4. Tumor tissue was analyzed by immunochemistry with antibodies specific for Ki-67 and MECA-32 (*brown staining*). No staining was observed in the naïve IgG control.

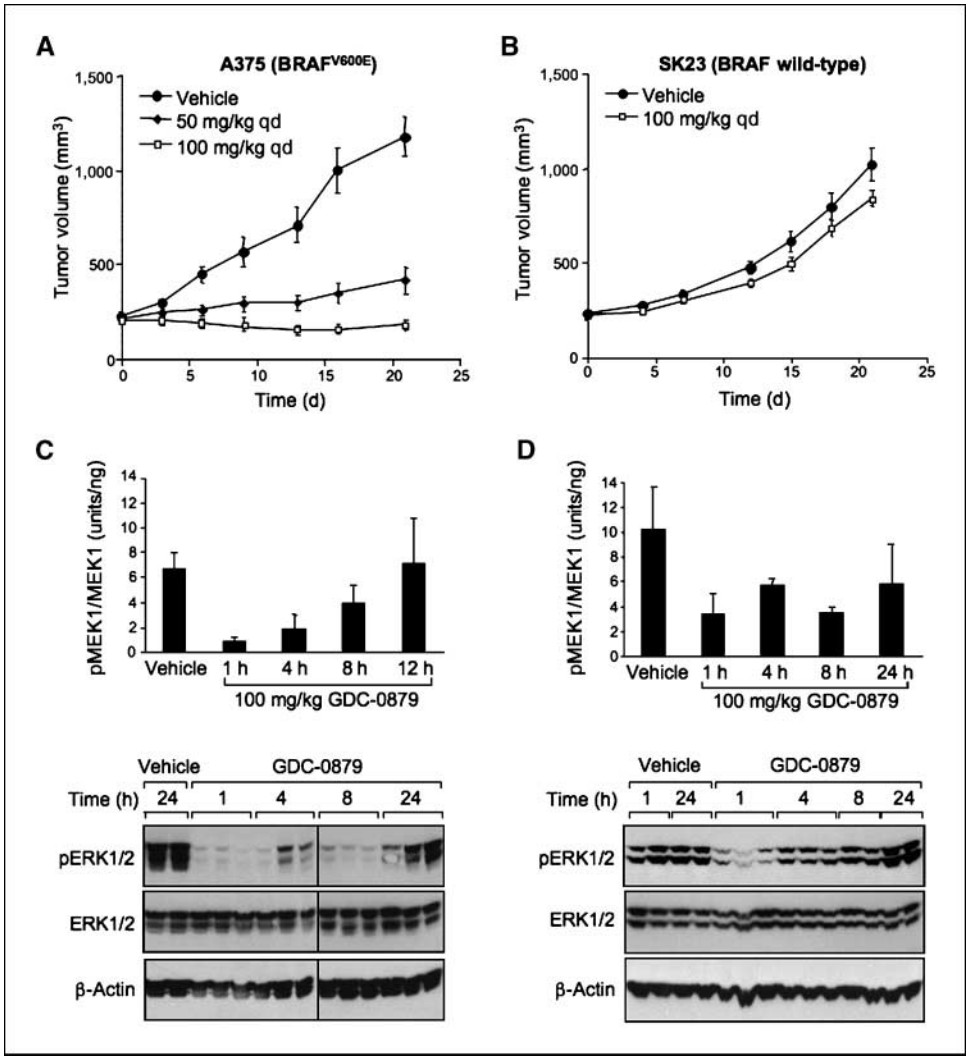

Figure 4. Wild-type BRAF melanoma tumors have an attenuated pharmacodynamic response to GDC-0879 treatment relative to $BRAF^{V600E}$ tumor xenografts. *A,* daily p.o. administration of 50 or 100 mg/kg GDC-0879 was highly efficacious in the $BRAF^{V600E}$ A375 tumor xenograft model. *B,* limited antitumor activity of GDC-0879 was observed for BRAF wild-type SK23 tumors. *Points,* mean for 10 tumor-bearing mice; *bars,* SE. *C,* additional groups of mice bearing 200- to 250-mm^3 A375 tumors were treated with a single dose of 100 mg/kg GDC-0879, and BRAF effector signaling was assessed in tumors either by quantitative ELISA for phosphorylated MEK1 (*top*) or immunoblot analysis of phosphorylated ERK1/2 (*pERK1/2*; *bottom*). Significant pharmacodynamic modulation was evident at 1, 4, and 8 h post-dose. Representative of three replicate experiments. *D,* GDC-0879–induced pharmacodynamic response was analyzed in SK23 tumor xenografts. The magnitude and duration of phospho-MEK1 (*top*) and phospho-ERK1/2 (*bottom*) inhibition were reduced in BRAF wild-type tumor tissue. Phospho-MEK1 ELISA data were normalized to total MEK1; *columns,* mean; *bars,* SD.

be sufficient to prevent melanoma tumor maintenance and progression in the context of oncogenic NRAS signaling.

As shown in Fig. 5*A*, an unexpected decrease in median tumor doubling time (LXFA 1041, $P = 0.002$; LXFA 983, $P = 0.1$) was observed for KRAS-mutant tumors following GDC-0879 treatment relative to control cohorts. End-of-study tumor volumes were also increased in response to GDC-0879 treatment (LXFA 1041, $P = 0.009$; LXFA 983, $P = 0.04$; data not shown). Given the negative interaction between GDC-0879 efficacy and KRAS mutation observed in these patient-derived non–small-cell lung cancer tumors, RAF effector signaling was investigated in tumor samples collected at 1, 8, or 24 hours after the final dose (Fig. 5*B*). Administration of GDC-0879 resulted in profound knockdown of phospho-ERK1/2 levels at both 1 and 8 hours post-dose in $BRAF^{V600E}$ tumors. In comparison, tumors with KRAS or NRAS mutation showed only a slight decrease in phospho-ERK1/2 at the 1-hour time point with a recovery of RAF effector signaling in <8 hours. Notably, phospho-ERK1/2 measured 8 hours after GDC-0879 treatment even significantly exceeded baseline levels in vehicle-treated control samples for some tumor models, such as LXFA 1041. Taken together, phospho-ERK1/2 is a suitable pharmacodynamic end point for tumor xenografts, and the magnitude (>90% inhibition) and duration (>8 hours) of signal reduction strongly correlate with the observed antitumor efficacy. Furthermore, transient elevation or "rebound" of ERK1/2 signaling resulting from GDC-0879 administration on a daily dosing schedule may lead to a cumulative increase in growth rate as observed for some non–small-cell lung cancer tumors with KRAS activating mutations.

Comparison of RAF and MEK inhibitors *in vitro* and *in vivo*. Given the limited responses observed for RAF inhibitors in BRAF wild-type tumors, we compared the activity of GDC-0879 with that of a known non–ATP-competitive inhibitor of MEK1/2 kinases, PD-0325901 (21). Initially, *in vivo* efficacy studies were done using the HCT116 tumor xenograft model ($KRAS^{G13D}$ genotype). Given that RAF kinases are direct upstream activators of MEK1/2 (1, 2), a similar efficacy might be expected from catalytic inhibition of either target. However, a dramatic difference in antitumor efficacy was observed for HCT116 tumors treated with either GDC-0879 or MEK inhibitor at their respective maximum tolerated doses (100 and 25 mg/kg daily; Fig. 6*A* and *B*). Whereas GDC-0879 treatment did not prevent the growth of established xenograft tumors, *in vivo* inhibition of MEK signaling resulted in a significant proportion of partial (20%) and complete (20%) tumor responses using this KRAS-mutant model (Fig. 6*B*). Interestingly, the antitumor activity of MEK inhibitor was correlated with strong (~ 90%) and sustained

(>6 hours) inhibition of phosphorylated ERK1/2 in this BRAF wild-type xenograft model (Supplementary Fig. S2).

To further compare the genotype-correlated sensitivities of RAF and MEK inhibitors, the compounds were profiled against a panel of 130 cell lines representing broad genetic heterogeneity and numerous tumor indications. The majority of GDC-0879–sensitive cell lines harbored BRAF mutations (24 of 35; Fig. 6*C*). As such, GDC-0879 activity was observed predominantly for tissues in which BRAF mutation is prevalent, such as melanoma and colorectal cancer (Supplementary Fig. S3*A*). MEK inhibitor treatment showed greater overall potency in $BRAF^{V600E}$ cells and was also effective in a significant proportion of KRAS-mutant (34 of 42) and BRAF/KRAS wild-type (23 of 61) tumor lines (Fig. 6*D*). As such, a strong inhibition of proliferation was noted for some tumor types in which KRAS mutation is uncommon, such as breast and prostate cancers (Supplementary Fig. S3*B*). Taken together, sensitivity to either BRAF or MEK inhibition is well correlated with BRAF mutation in tumor cell lines; however, only MEK inhibition is effective in preventing tumor cell growth in the context of wild-type BRAF. It is encouraging that the possible clinical utility of MEK inhibitors may be broader than originally suggested from studies using a much smaller cell line panel (21). The molecular features that distinguish the MEK inhibitor–sensitive and MEK inhibitor–resistant subsets of either oncogenic KRAS–expressing or KRAS/BRAF wild-type cells are currently not well understood and further elucidation is required.

Discussion

We describe here the properties of GDC-0879 and compound 2a, orally bioavailable RAF family kinase inhibitors that exhibit robust single-agent activity *in vitro* and *in vivo*. Because previous efforts to validate the role of BRAF in oncogenesis have typically relied on nonselective kinase inhibitors (11) or RNA interference approaches to induce a steady-state suppression of MEK-ERK signaling (22), the objective of our study was to provide quantitative information on the kinetics of pathway suppression required for antitumor efficacy. In contrast to other published reports of RAF-selective compounds (12, 13), we correlated the efficacy of GDC-0879 with proximal (substrate phosphorylation) and distal (tumor cell proliferation) pharmacodynamic biomarkers. Phospho-MEK1/2 and phospho-ERK1/2 were validated as pharmacodynamic end points, and the extent (>90%) and duration (>8 hours) of pathway inhibition were shown to correlate with *in vivo* efficacy in a variety of preclinical models (Figs. 4 and 5).

The contribution of RAS/RAF mutational status to *in vitro* and *in vivo* efficacy was also extensively investigated. The signaling mechanism to explain the potent cellular activity of MEK inhibition

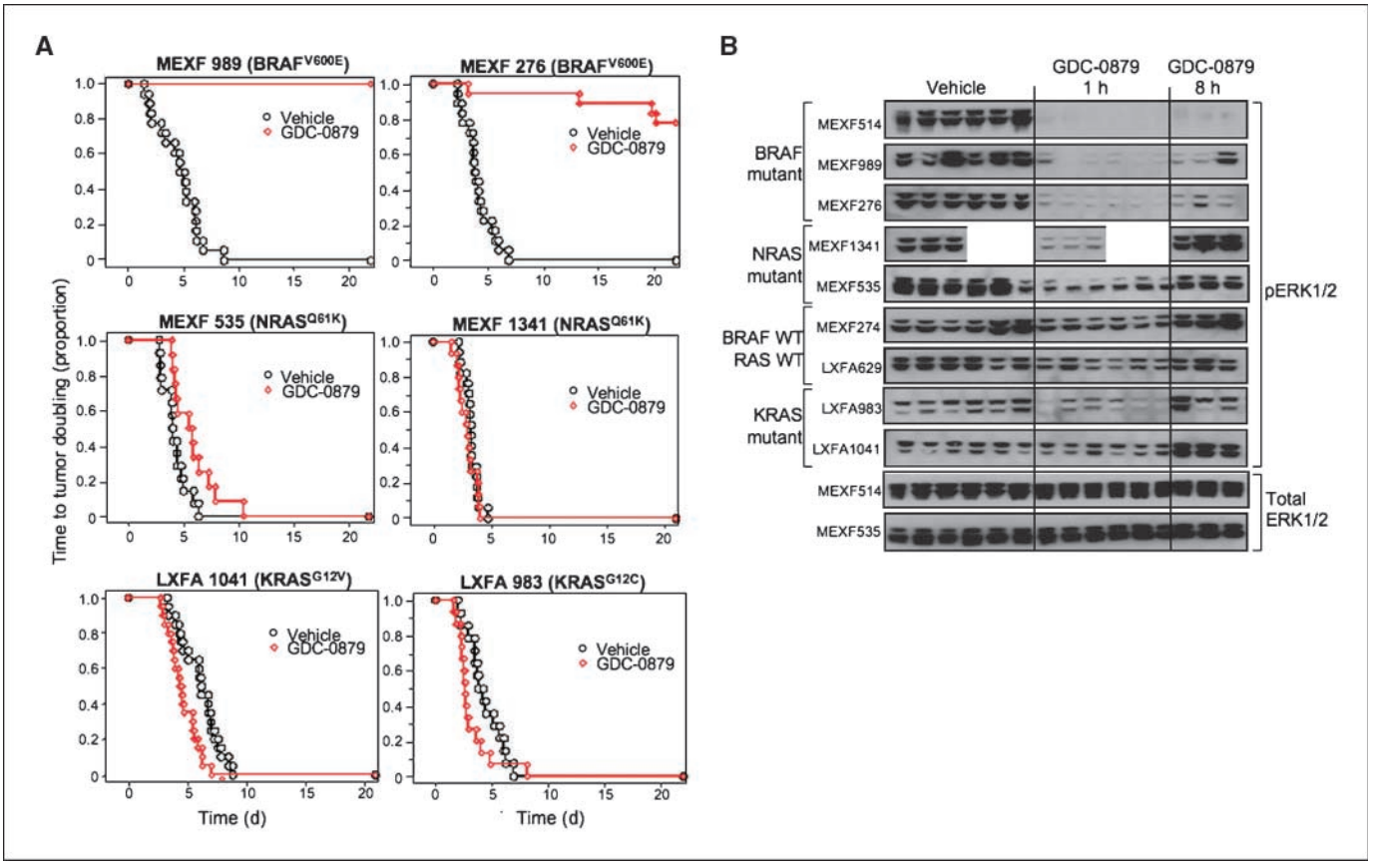

Figure 5. Duration and extent of BRAF pathway inhibition determines GDC-0879 efficacy in primary human tumor xenograft models. *A,* Kaplan-Meier plot showing time to tumor doubling for patient-derived melanoma and non–small cell lung cancer tumor models treated daily with 100 mg/kg GDC-0879 or vehicle. Genotypes for BRAF, NRAS, and KRAS are indicated. A statistically significant ($P < 0.05$) delay in tumor progression was noted for MEXF 989, MEXF 276, and MEXF 535 tumors. GDC-0879 administration significantly accelerated growth of some KRAS-mutant non–small cell lung cancer tumors, such as LXFA 1041 and LXFA 983. *B,* GDC-0879 treatment down-regulated ERK1/2 phosphorylation in $BRAF^{V600E}$ primary human xenograft tumors. In time course pharmacodynamic studies, mice were treated with 100 mg/kg GDC-0879 and sacrificed at 1 or 8 h following the last dose (days 21–24). Immunoblots of phosphorylated and total ERK1/2 are shown. Potent phospho-ERK1/2 inhibition sustained through 8 h was strongly correlated with $BRAF^{V600E}$ status and GDC-0879 antitumor efficacy. Total ERK1/2 expression was examined in all samples as a loading control.

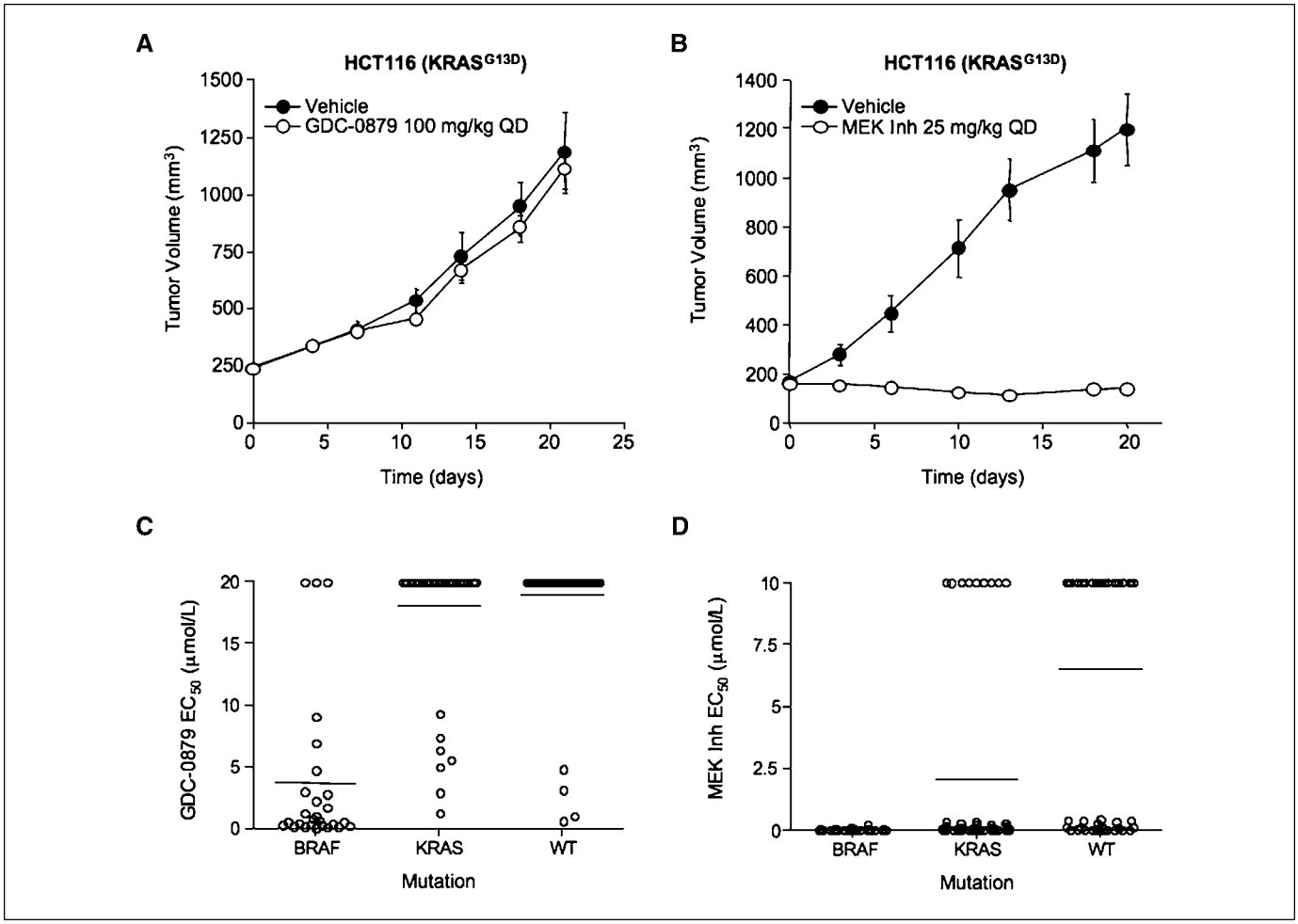

Figure 6. KRAS-mutant tumor cell lines show differential sensitivity to GDC-0879 RAF and MEK inhibitors *in vivo* and *in vitro*. *A* and *B,* inhibition of MEK, but not RAF, prevented the *in vivo* growth of KRAS-mutant HCT116 tumors. Mice were randomized when tumors reached ~200 mm^3 and treatment was initiated with either 100 mg/kg GDC-0879 (*A*) or 25 mg/kg MEK inhibitor (*MEK Inh*; *B*) on a daily schedule. *Points,* mean; *bars,* SE. *C,* GDC-0879 EC_{50} values for 130 cell lines are shown as a function of BRAF and KRAS mutational status. GDC-0879–mediated inhibition of cell growth was strongly correlated with BRAF mutation. *D,* dot plots for MEK inhibitor EC_{50} values are organized according to genotype. MEK inhibition was also potent on a significant fraction of cell lines expressing wild-type BRAF. Data represent the mean of quadruplicate measurements.

on cells that are resistant to RAF inhibitors is currently not understood. Surprisingly, our *in vivo* efficacy studies with patient-derived non–small-cell lung cancer tumors showed that some KRAS-mutant tumors not only failed to show an antitumor benefit from GDC-0879 but even exhibited accelerated tumor growth (Fig. 5*A*). A possible negative interaction between GDC-0879 and KRAS mutation requires further investigation and should be viewed cautiously until confirmatory *in vivo* data using complementary model systems are available. It is interesting, however, to speculate on the molecular mechanisms behind the observed posttreatment rebound of elevated phospho-ERK1/2 signaling (Fig. 5*B*). It is possible that transient RAF inhibition may alter oncogenic KRAS signaling by triggering the extensive network of positive and negative regulatory loops that feed into the RAF/MEK/ERK kinase cascade. For instance, temporal modulation of RAS signaling can occur via induction of members of the MAPK phosphatase or SPROUTY protein families (23, 24) or via direct feedback phosphorylation to negatively regulate the association of RAF1-RAS and SOS-GRB2 protein complexes (25, 26). In this way, RAS-mediated cellular responses have been shown to be context dependent and affected by the prior exposure of a cell to signaling stimuli and inhibitors (27). This feedback mechanism may be important in the context of transient pathway inhibition resulting from intermittent delivery of small-molecule inhibitors with high C_{max} exposure and rapid *in vivo* clearance.

RAF inhibitors were also shown to exhibit strong selectivity toward tumor cells expressing oncogenic BRAF (Figs. 2*A* and 6*C*) and particular tumor types, such as melanoma, colon cancer, and ovarian cancer (Fig. 6*D*). *In vivo* data for GDC-0879 treatment of both cell line– and patient tumor–derived preclinical models further support the trend of $BRAF^{V600E}$ oncogene addiction (Supplementary Tables S3 and S4). Importantly, the sensitivity of tumor cells to RAF inhibition was inversely correlated with PI3K activation, and combined treatment of GDC-0879 and GDC-0941 effectively decreased the viability of melanoma cells having both oncogenic $BRAF^{V600E}$ and PTEN deficiency (Fig. 2*B* and *C*). These data provide a strong rationale for therapeutic combinations in the clinic. Lastly, given the observed genotype-correlated drug sensitivities, selection of the appropriate patient population is a major issue facing the development of both RAF and MEK

inhibitors. Our data suggest that a priori analysis of biopsy tumor material for RAS/BRAF genotype (Fig. 6) or expression signatures of response (Fig. 1*B*) will help stratify patients most likely to benefit from RAF inhibitor therapy.

Disclosure of Potential Conflicts of Interest

All authors are employees of Genentech, Inc.

Acknowledgments

Received 9/16/08; revised 12/19/08; accepted 1/14/09; published OnlineFirst 3/10/09.

The costs of publication of this article were defrayed in part by the payment of page charges. This article must therefore be hereby marked *advertisement* in accordance with 18 U.S.C. Section 1734 solely to indicate this fact.

We thank the medicinal chemistry group at Array Biopharma for supplying RAF inhibitors; Harvey Wong and Georgia Hatzivassiliou for helpful discussions; and Jeffrey Wallin, Peter Haverty, Kyle Edgar, Jane Guan, Christine Orr, Bijay Jaiswal, Jeffrey Eastham-Anderson, and the Genentech Histology and immunohistochemistry core labs for technical support.

References

1. Sebolt-Leopold JS, Herrera R. Targeting the mitogen-activated protein kinase cascade to treat cancer. Nat Rev Cancer 2004;4:937–47.
2. Wellbrock C, Karasarides M, Marais R. The RAF proteins take centre stage. Nat Rev Mol Cell Biol 2004;5:875–85.
3. Davies H, Bignell GR, Cox C, et al. Mutations of the BRAF gene in human cancer. Nature 2002;417:949–54.
4. Yuen ST, Davies H, Chan TL, et al. Similarity of the phenotypic patterns associated with BRAF and KRAS mutations in colorectal neoplasia. Cancer Res 2002;62:6451–5.
5. Wan PT, Garnett MJ, Roe SM, et al. Mechanism of activation of the RAF-ERK signaling pathway by oncogenic mutations of B-RAF. Cell 2004;116:855–67.
6. Zhang BH, Guan KL. Activation of B-Raf kinase requires phosphorylation of the conserved residues Thr598 and Ser601. EMBO J 2000;19:5429–39.
7. Yazdi AS, Palmedo G, Flaig MJ, et al. Mutations of the BRAF gene in benign and malignant melanocytic lesions. J Invest Dermatol 2003;121:1160–2.
8. Sumimoto H, Miyagishi M, Miyoshi H, et al. Inhibition of growth and invasive ability of melanoma by inactivation of mutated BRAF with lentivirus-mediated RNA interference. Oncogene 2004;23:6031–9.
9. Hoeflich KP, Gray DC, Eby MT, et al. Oncogenic BRAF is required for tumor growth and maintenance in melanoma models. Cancer Res 2006;66:999–1006.
10. Michaloglou C, Vredeveld LC, Mooi WJ, Peeper DS. BRAF(E600) in benign and malignant human tumours. Oncogene 2008;27:877–95.
11. Wilhelm SM, Carter C, Tang L, et al. BAY 43–9006 exhibits broad spectrum oral antitumor activity and targets the RAF/MEK/ERK pathway and receptor tyrosine kinases involved in tumor progression and angiogenesis. Cancer Res 2004;64:7099–109.
12. King AJ, Patrick DR, Batorsky RS, et al. Demonstration of a genetic therapeutic index for tumors expressing oncogenic BRAF by the kinase inhibitor SB-590885. Cancer Res 2006;66:11100–5.
13. Tsai J, Lee JT, Wang W, et al. Discovery of a selective inhibitor of oncogenic B-Raf kinase with potent antimelanoma activity. Proc Natl Acad Sci U S A 2008;105:3041–6.
14. Hansen JD, Grina J, Newhouse B, et al. Potent and selective pyrazole-based inhibitors of B-Raf kinase. Bioorg Med Chem Lett 2008;18:4692–5.
15. Dunnett CW, Crisafio R. The operating characteristics of some official weight variation tests for tablets. J Pharm Pharmacol 1955;7:314–27.
16. Cummings J, Zelcer N, Allen JD, et al. Glucuronidation as a mechanism of intrinsic drug resistance in colon cancer cells: contribution of drug transport proteins. Biochem Pharmacol 2004;67:31–9.
17. Halilovic E, She QB, Ye Q, Solit DB, Rosen N. Coexistent PI3K mutation in human tumors is associated with decreased dependency on mutant KRAS and MEK/ERK signaling for transformation. AACR Annual Meeting 2008;abstract 4938.
18. Folkes AJ, Ahmadi K, Alderton WK, et al. The identification of 2-(1*H*-indazol-4-yl)-6-(4-methanesulfonyl-piperazin-1-ylmethyl)-4-morpholin-4-yl-thieno[3,2-d]pyrimidine (GDC-0941) as a potent, selective, orally bioavailable inhibitor of class I PI3 kinase for the treatment of cancer. J Med Chem 2008;51:5522–32.
19. Ross DT, Scherf U, Eisen MB, et al. Systematic variation in gene expression patterns in human cancer cell lines. Nat Genet 2000;24:227–35.
20. Fiebig HH. Comparison of tumor response in nude mice and in the patients. In: Winograd B, Pinedo H, editors. Human tumor xenografts in anticancer drug development. Berlin: Springer; 1988. p. 25–30.
21. Solit DB, Garraway LA, Pratilas CA, et al. BRAF mutation predicts sensitivity to MEK inhibition. Nature 2006;439:358–62.
22. Sharma A, Trivedi NR, Zimmerman MA, Tuveson DA, Smith CD, Robertson GP. Mutant V599EB-Raf regulates growth and vascular development of malignant melanoma tumors. Cancer Res 2005;65:2412–21.
23. Bhalla US, Ram PT, Iyengar R. MAP kinase phosphatase as a locus of flexibility in a mitogen-activated protein kinase signaling network. Science 2002;297:1018–23.
24. Mason JM, Morrison DJ, Basson MA, Licht JD. Sprouty proteins: multifaceted negative-feedback regulators of receptor tyrosine kinase signaling. Trends Cell Biol 2006;16:45–54.
25. Dougherty MK, Muller J, Ritt DA, et al. Regulation of Raf-1 by direct feedback phosphorylation. Mol Cell 2005;17:215–24.
26. Douville E, Downward J. EGF induced SOS phosphorylation in PC12 cells involves P90 RSK-2. Oncogene 1997;15:373–83.
27. Ingolia NT, Murray AW. Signal transduction. History matters. Science 2002;297:948–9.